Communications in Physics, Vol. 36, No. 1 (2026), pp. 19-26
DOI: https://doi.org/10.15625/0868-3166/23350

Metal-insulator transitions in the two dimensional ionic Hubbard model within coherent potential approximation

Nguyen Thi Hai Yen and Hoang Anh Tuan[†]

Institute of Physics, Vietnam Academy of Science and Technology,
10 Dao Tan, Giang Vo, Hanoi, Vietnam

E-mail: [†]hatuan@iop.vast.vn

Received 28 August 2025
Accepted for publication 28 November 2025
Published 5 March 2026

Abstract. *We employ the coherent potential approximation to investigate the phase diagram of the ionic Hubbard model on the square lattice. The results show the existence of two insulating phases: a band insulator in the regime of large ionic potential Δ and small Coulomb interaction U, and a Mott insulator in the regime of large U. Between these two insulating phases, a metallic phase emerges as an intermediate state. The obtained phase diagram is compared to those on the Bethe lattice.*

Keywords: ionic Hubbard model; metal-insulator transition; dynamic mean field theory.
Classification numbers: 71.10.Fd; 71.30.+h; 71.27.+a.

1. Introduction

Electron-electron interactions are crucial for understanding many complex phenomena like magnetism, superconductivity, and Mott insulators. These correlations often lead to emergent behaviors that cannot be explained by non-interacting electron models, deepening our understanding of the collective behavior in materials. To describe and explain the physics of narrow band correlated materials, including the Mott insulator, the Hubbard model was proposed [1]. The ionic Hubbard model (IHM) is an extension of the standard Hubbard model, incorporating a staggered potential that mimics the presence of ions with different charges in a lattice. It's particularly useful for studying systems where sub-lattices experience different onsite energies, such as ionic compounds or materials with alternating ionic potentials [2].

The phase diagram of the ionic Hubbard model at half-filling has been intensively studied in various dimensions by a lot of techniques [3,4]. In one dimension (1D) it features a competition between band insulator (BI), Mott insulator (MI), and possibly a spontaneously dimerized phase [3, 4]. In the infinite-dimensional limit, in the paramagnetic sector many studies have found a metallic phase sandwiched between the band and the Mott insulating phases [5–8].

In the two-dimensional (2D) case, the situation is much less convincing. Using cluster dynamical mean field theory (CDMFT), Kancharla and Dogotto [9] found a bond-ordered phase appearing between the band and Mott insulating phases. Chen et al [10] obtained similar results using the variational cluster approach (VCA). On the other hand, by means of determinant quantum Monte Carlo (QMC), Paris et al [11] and Bouadim et al [12] pointed to the presence of a metallic phase intervening between the BI and MI phases. Similar findings were found by Shabazy and Ebrahimkhas within the DMFT [13]. Using exact diagonalization and QMC Cho and Lee [14] suggested that the intervening metallic region will shrink to a quantum critical point as temperature decreases to zero.

The purpose of this paper is twofold. First, we study the phases of the half-filled ionic Hubbard model on a two-dimensional square lattice using the coherent potential approximation (CPA). Second, we consider the effect of different lattices, the square and the Bethe lattice, on the resulting phase diagrams. It is well known that the CPA is a widely used theoretical method for studying the electronic properties of disordered materials and the metal–insulator transitions of many-body systems. In particular, it is well suited for deriving the phase diagram of the half-filled ionic Hubbard model on the Bethe lattice [7]. In the next Sec. 2, we introduce our model and theoretical formulation. In Sec. 3, the results of CPA phase diagram and the staggered charge density are calculated and discussed. The final section contains a short summary.

2. Models and methods

The IHM on a bipartite lattice (sub-lattices A and B) square lattice is given by the following Hamiltonian:

$$H = -t \sum_{i\in A, j\in B,\sigma} [c^{+}_{i\sigma} c_{j\sigma} + \text{H.c.}] + U \sum_{i} n_{i\uparrow} n_{i\downarrow} + \varepsilon_A \sum_{i\in A} n_i + \varepsilon_B \sum_{i\in B} n_i - \mu \sum_{i} n_i, \tag{1}$$

where t denotes the nearest neighbor hopping parameter, $c_{i\sigma}(c^{+}_{i\sigma})$ annihilates (creates) an electron with spin σ at site i, $n_{i\sigma} = c^{+}_{i\sigma} c_{i\sigma}$ and $n_i = n_{i\uparrow} + n_{i\downarrow}$. U denotes the on-site Coulomb repulsion, $\varepsilon_A = \Delta$ and $\varepsilon_B = -\Delta$ the ionic staggered potential in sub-lattice A and B, respectively. The chemical potential is $\mu = U/2$ at half-filling.

Within the alloy-analogue approximation the Hamiltonian (1) is replaced by an effective one-electron Hamiltonian:

$$\tilde{H} = \sum_{i\in A,\sigma} E_{A\sigma} n_{i\sigma} + \sum_{i\in B,\sigma} E_{B\sigma} n_{i\sigma} - t \sum_{i\in A, j\in B,\sigma} [c^{+}_{i\sigma} c_{j\sigma} + \text{H.c.}], \tag{2}$$

where the disorder potential $E_{\alpha,\sigma}$ takes the values

$$E_{\alpha,\sigma} = \begin{cases} \varepsilon_\alpha - U/2 & \text{with probability } 1 - n_{\alpha,-\sigma}, \\ \varepsilon_\alpha + U/2 & \text{with probability } n_{\alpha,-\sigma}. \end{cases} \tag{3}$$

Here $\alpha = A, B$. The average occupation $n_{\alpha,\sigma}$ must be determined self-consistently. In this paper, we focus on the paramagnetic sector, for which $n_{\alpha,\uparrow} = n_{\alpha,\downarrow} = n_\alpha/2$. As a result, all the one-electron quantities become spin-independent.

In the CPA method, the disorder potential $E_{\alpha,\sigma}$ can be replaced by a local self-energy $\Sigma_\alpha(\omega)$, then the local Green function in the bipartite lattice takes the form [15]

$$G_\alpha(\omega) = (\omega - \Sigma_{\bar{\alpha}}) \int \frac{\rho_0(E)dE}{(\omega - \Sigma_A)(\omega - \Sigma_B) - E^2}, \tag{4}$$

where $\alpha = A(B)$ and $\bar{\alpha} = B(A)$, $\rho_0(E)$ is the bare density of states (DOS) of the square lattice

$$\rho_0(E) = \frac{1}{2\pi^2 t}\int_0^\pi dk_x \int_0^\pi dk_y \delta(\tilde{\epsilon} + \cos k_x + \cos k_y) = \frac{1}{2\pi^2 t}\int_{-1}^{1} \frac{dx}{\sqrt{(1-x^2)(1-(\tilde{\epsilon}+x)^2)}}, \tag{5}$$

where $\tilde{\epsilon} = E/2t$. On the other hand, the Green function of effective medium described by the Hamiltonian (2) has to be averaged over all possible disorder configuration of the random potential:

$$\tilde{G}_\alpha(\omega) = \frac{(1-n_\alpha/2)G_\alpha(\omega)}{1-(\varepsilon - U/2 - \Sigma_\alpha(\omega))G_\alpha(\omega)} + \frac{(n_\alpha/2)G_\alpha(\omega)}{1-(\varepsilon + U/2 - \Sigma_\alpha(\omega))G_\alpha(\omega)}. \tag{6}$$

The CPA requires that the averaged Green function of effective medium be identical to the local Green function

$$\tilde{G}_\alpha(\omega) = G_\alpha(\omega). \tag{7}$$

The equations (4)-(7) need to be solved with $n_A + n_B = 2$, where at zero temperature $n_\alpha = -\frac{2}{\pi}\int_{-\infty}^{0} \mathrm{Im}\, G_\alpha(\omega)d\omega$. Then the local DOS $\rho_\alpha(\omega) = -\mathrm{Im}\, G_\alpha(\omega)/\pi$ and the staggered charge density $n_B - n_A$ can be determined as a function of the model parameters U and Δ. A metallic phase is characterized by non-zero total DOS at the Fermi level $\rho(0) = \sum_\alpha \rho_\alpha(0)$. A Mott insulator is distinguished from a band insulator by the small value of the staggered charge density, in particular for $U \gg \Delta$ one has $n_A \approx n_B \approx 1$.

3. Results and discussion

The equations (4) - (7) are numerically solved self-consistently to determine the self-energy and the Green function.

For the 2D square lattice, the local Green function at a lattice site cannot be evaluated analytically as in the Bethe lattice (see Eq. (4) in [7]). Instead, we compute the integral in Eqs. (5) and (4) directly. Note that in the integration of Eq. (5) the limits of the DOS integration for the square lattice are chosen such that the denominator remains well-defined. Finally, in Eq. (4) the integration bounds are taken from $-4t$ to $4t$. To start a self-consistent loop, we select an initial value for the self-energy (usually set to zero) for sublattices A and B. These values are substituted into equation (4) to calculate the local Green function of the square lattice. The resulting local Green functions are then substituted into the right-hand side of equation (6) to obtain the CPA Green function. Finally, the new self-energy is determined by: $\Sigma_\alpha(\omega) = \Sigma_\alpha(\omega) + 1/G_\alpha(\omega) - \tilde{G}_\alpha(\omega)$. In the numerical calculations, we use $\omega + i\eta$ instead of real-frequency ω. The parameter η is chosen as a small positive number, typically in the range 10^{-3} to 10^{-2} to ensure the convergence of the self-consistent equations. In order to determine the phase boundaries, we compute the local

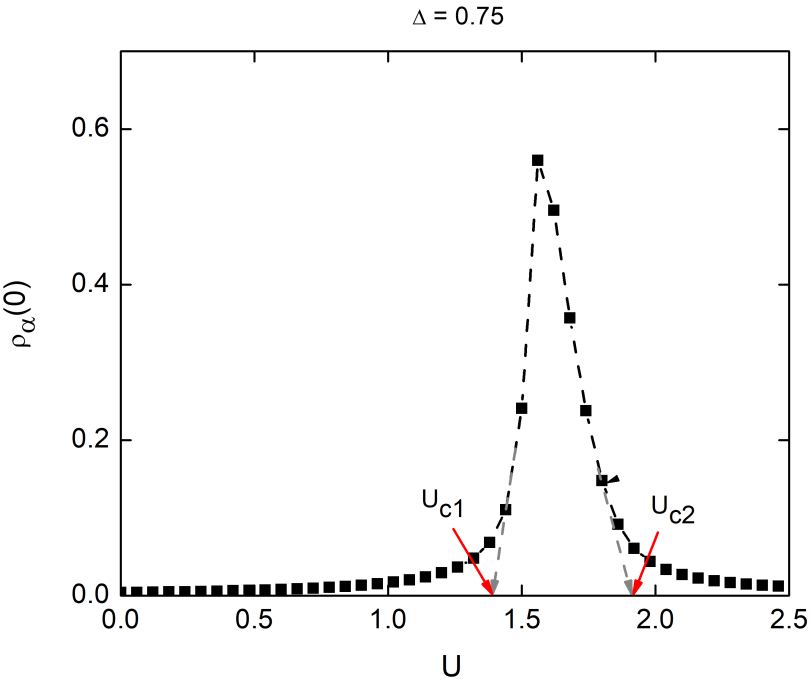

Fig. 1. Local DOS at the Fermi level for $\Delta = 0.75$ as a function of Coulomb interaction U. Spline extrapolation to $\eta \to 0^+$ was used to obtain the critical interactions $U_{c1} \approx 1.41$ and $U_{c2} \approx 1.91$. Energy scale: $W = 4t = 1$.

DOS at the Fermi level $\rho_{A/B}(0)$. In Fig. 1 $\rho_\alpha(0)$ as a function of the Coulomb interaction U for $\Delta = 0.75$ is presented. Throughout this paper, half the bandwidth $W = 4t$ is chosen as the unit of energy. To reach the limit $\eta \to 0^+$ we use a simple linearly extrapolation. We notice that the critical interaction values obtained are consistent, regardless of the extrapolation scheme, linearly or polynomial, were used. Then from the data for $U > U_1^* = 1.45$ and the data for $U < U_2^* = 1.8$ we obtain the critical interactions $U_{c1} \approx 1.41$ and $U_{c2} \approx 1.91$, respectively. The results show that the system undergoes two continuous (second-order) phase transitions: first, at small $U < U_{c1}$, the system is in a band-insulating phase; as the Coulomb interaction U increases to the critical value U_{c1}, the system gradually enters a metallic phase. Finally, at a larger Coulomb interaction $U > U_{c2}$, the system stabilizes the Mott-insulating phase.

In Fig. 2 we plot the local DOS for both sub-lattices A and B for $\Delta = 0.75$ and for three values of U. Due to particle-hole symmetry at half-filling we obtain $\rho_A(\omega) = \rho_B(-\omega)$. For $U = 0.5$ and 2.5 the DOS at the Fermi level ($\omega = 0$) equals zero, which indicates that the system is an insulator. It can be seen that $n_B \gg n_A$ for $U = 0.5$ while $n_B \approx n_A$ for $U = 2.5$. Hence, the system for $U = 0.5$ and 2.5 corresponds to BI and MI phases, respectively. In contrast, the result of DOS for $U = 1.7$ clearly shows a metallic phase in the system.

The main result of our study is the phase diagram of the square lattice for the ionic Hubbard model at half-filling at zero temperature shown in Fig. 3.

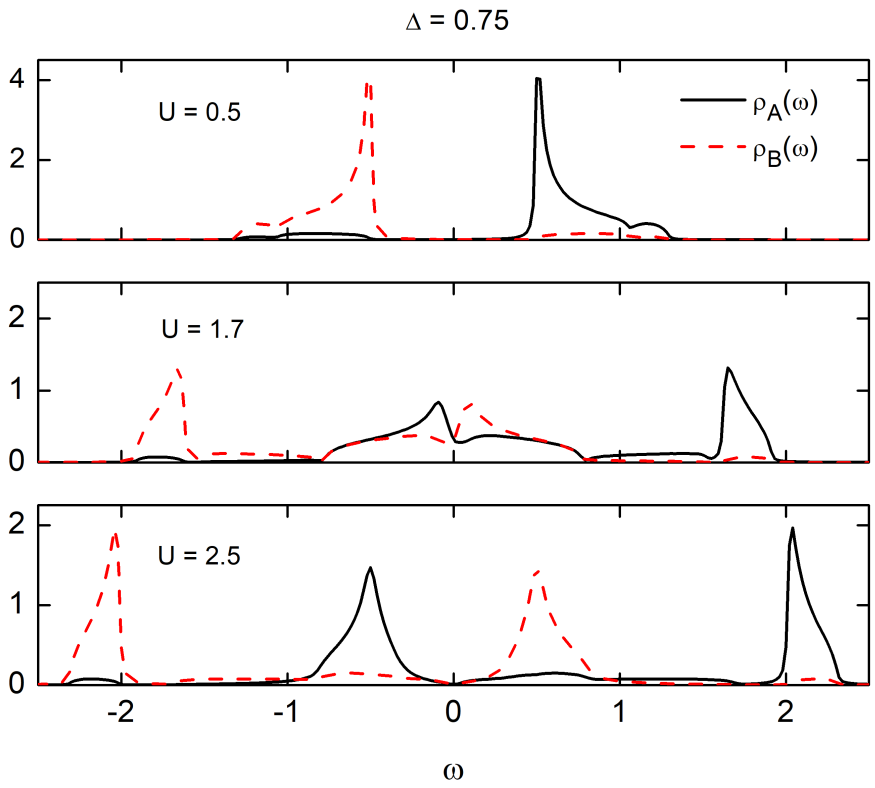

Fig. 2. Local DOS for both sub-lattices for $\Delta = 0.75$ for Coulomb interaction $U = 0.5, 1.7$ and 2.5. Top panel: a band insulator state for $U = 0.5$; Center panel: a metallic state at $U = 1.7$; Bottom panel: a Mott insulator state for $U = 2.5$.

The metallic phase is between the BI and MI phases. We plotted the phase diagram of the Bethe lattice [7] in comparison with the square lattice. It can be seen that the phase boundary between the metallic and band insulator phases of the square lattice is almost coincide with the line $U = 2\Delta$ and is therefore slightly lower than those of the Bethe lattice. In contrast, the phase boundary between the metallic and Mott insulator phases of the square lattice is significantly raised from those of the Bethe lattice for the small values of Δ. The DOS of the square lattice has a Van-Hove singularity around the Fermi level, so in IHM for small Δ the DOS near the Fermi level of the square lattice is larger than that of the Bethe lattice. This results in the metal region in the square lattice being larger than the metal region in the Bethe lattice. However, for $\Delta \gg 1$ the metallic region in both diagrams becomes very small. We note that in [16] Rowlands and Yu-Zhong Zhang compared the Bethe lattice results in [7] with the 2D lattice results without using the bare DOS in Eq. (5), they focused on the differences introduced by including spatial correlations between sites into the CPA. While in this paper, we clarify the impact of the used bare DOS on the obtained results. Compared to the results of Shabazy and Ebrahimkhas in DMFT [13], the shape of the metal region in our scheme is different for small Δ (e.g. for $\Delta = 0$ in our CPA calculation $U_{c2} \approx 6t$ while it equals $9.1t$ in [13]), but in both phase diagrams it shrinks to a line as Δ increases. On

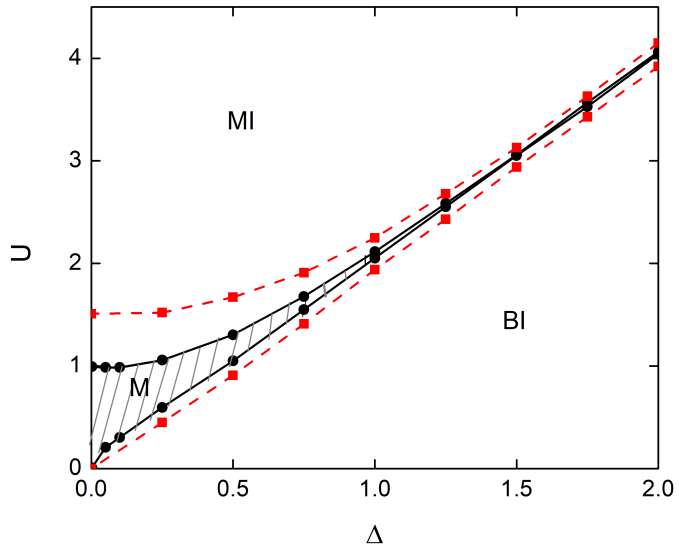

Fig. 3. Phase diagram of ionic Hubbard model for the 2D square lattice (red-dash lines) and for the Bethe lattice (circle - solid lines). BI, M, and MI symbols corresponding to Band Insulator, Metal, and Mott Insulator phases. The cross-hatched area indicates metallic region for the Bethe lattice using CPA in Ref. [7].

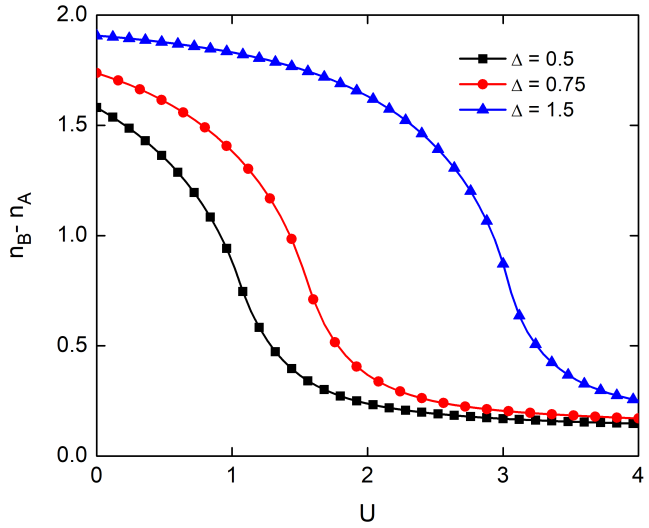

Fig. 4. Staggered density $n_B - n_A$ as a function of the Coulomb interaction at ionic energies $\Delta = 0.5, 0.75$ and 1.5. The change in slope occurs near $U = 2\Delta$, signaling the transition from band insulator to metal, and phase transitions BI-M-MI are found to be continuous.

the other hand, in the DMFT and CPA phase diagrams the metallic region extends to the $\Delta = 0$ line, whereas in the QMC phase diagram the metallic phase is only present when U and Δ both

nonzero. Furthemore, it is unclear whether its region disappears for large Δ. The limited sizes and finite temperature used in QMC may be the reasons for these differences.

Figure 4 shows the staggered charge density $n_B - n_A$ as a function of U for three values of Δ. The curves for the square lattice are similar to those in the Bethe lattice [7]: for a fixed Δ it decreases as U increases and approaches zero for $U \to \infty$; the change in slope occurs near $U = 2\Delta$, signaling the transition from band insulator to metal; and the BI-M-MI phase transitions are found to be continuous, consistent with the results in [12], but in contrast to those in [9], providing a first-order transition between the intermediate phase and the Mott insulator. The transition from band insulator to metal just after $U = 2\Delta$, achieved by applying CPA in a 2D model, which is not yet available in QMC and DMFT studies. From the curve for $\Delta = 0.75$ one can estimate $n_B - n_A \approx 1.6$ for $U = 0.5$ (band insulator) and $n_B - n_A \approx 0.24$ for $U = 2.5$ (Mott insulator) as mentioned earlier.

4. Conclusion

We have studied quantum phase transitions in the half-filled ionic Hubbard model on a 2D square lattice using the CPA method. Our results show that a metallic phase is sandwiched between the band insulator and Mott insulator phases. Compared to the phase diagram of the Bethe lattice [7], we see that the shape of the metallic region is similar but larger, and the difference decreases with increasing Δ. As in [7,12], in our calculations the metal–insulator phase transitions are continuous. The similar overall shape of the phase diagrams as well as the staggered charge density curves obtained from the Bethe lattice and from the 2D square lattice shows that in the CPA they are qualitatively independent of the choice of the used bare DOS. Similar conclusions are found from the results of DMFT calculations with the IPT impurity solver [5,13]. We note that the predictions of metal-insulator transition due to local potential and electron correlation in the 2D IHM can be experimentally verified through studying the evolution of the electronic structure in $SrRu_{1-x}Ti_xO_3$ as a function of x using high resolution photoemission spectroscopy [17]. Here we only consider the paramagnetic sector, however, as noted in [18], the physical picture of the Mott metal-insulator transition of DMFT and CPA on the Bethe lattice can change significantly in two dimensions due to strong, spatially extended antiferromagnetic correlations. This issue requires further study using more sophisticated methods and we will leave it for the future.

Acknowledgment

This research is supported by Vietnam Academy of Science and Technology under Program NVCC05.01/25-25.

References

[1] J. Hubbard, *Electron correlations in narrow energy bands*, Proc. R. Soc. A **276** (1963) 238.
[2] T. Egami, S. Ishihara and M. Tachiki, *Lattice effect of strong electron correlation: implication for ferroelectricity and superconductivity*, Science **261** (1993) 1307.
[3] M. Fabrizio, A. O. Gogolin and A. A. Nersesyan, *From band insulator to Mott insulator in one dimension*, Phys. Rev. Lett. **83** (1999) 2014.
[4] C. D. Batista and A. A. Aligia, *Exact bond ordered ground state for the transition between the band and the Mott insulator*, Phys. Rev. Lett. **92** (2004) 246405.
[5] A. Garg, H. R. Krishnamurthy and M. Randeria, *Can correlations drive a band insulator metallic?*, Phys. Rev. Lett. **97** (2006) 046403.

[6] K. Byczuk, M. Sekania, W. Hofstetter and A. P. Kampf, *Insulating behavior with spin and charge order in the ionic Hubbard model*, Phys. Rev. B **79** (2009) 121103.
[7] A. T. Hoang, *Metal-insulator transitions in the half-filled ionic Hubbard model*, J. Phys.: Condens. Matter **22** (2010) 095602.
[8] A. G. S. Bag and H. R. Krishnamurthy, *Phase diagram of the half-filled ionic Hubbard model*, Phys. Rev. B **91** (2015) 235108.
[9] S. S. Kancharla and G. Dagotto, *Correlated insulated phase suggests bond order between band and Mott insulators in two dimensions*, Phys. Rev. Lett. **98** (2007) 016402.
[10] H.-M. Chen, H. Zhao, H.-Q. Lin and C.-Q. Wu, *Bond-located spin density wave phase in the two-dimensional (2D) ionic Hubbard model*, New J. Phys. **12** (2010) 093021.
[11] N. Paris, K. Bouadim, F. Hebert, G. G. Batrouni and R. T. Scalettar, *Quantum monte carlo study of an interaction-driven band-insulator–to–metal transition*, Phys. Rev. Lett. **98** (2007) 046403.
[12] K. Bouadim, N. Paris, F. Hébert, G. G. Batrouni and R. T. Scalettar, *Metallic phase in the two-dimensional ionic Hubbard model*, Phys. Rev. B **76** (2007) 085112.
[13] A. Shahbazy and M. Ebrahimkhas, *Quantum phase transitions in the two dimensional ionic-Hubbard model*, Chinese J. Phys. **58** (2019) 273.
[14] J. Cho and J. Lee, *Exact diagionalization and quantum Monte Carlo study of an ionic Hubbard model in two dimensions*, J. Korean Phys. Soc. **70** (2017) 494.
[15] A.-T. Hoang, T.-H.-Y. Nguyen and D.-A. Le, *Electronic phase diagram in the half-filled ionic Hubbard model with site-dependent interactions*, Physica B: Conden. Matter **531** 110.
[16] D. A. Rowlands and Y. Z. Zhang, *Inclusion of intersite spartial correlation in the alloy analogy approach to the half-filled ionic Hubbard model*, J. Phys.: Condens. Matter **27** (2014) 274210.
[17] K. Maiti, R. S. Singh and V. R. R. Medicherla, *Evolution of a band insulating phase from a correlated metallic phase*, Phys. Rev. B **76** (2007) 165128.
[18] T. Schäfer, F. Geles, D. Rost, G. Rohringer, E. Arrigoni, K. Held *et al.*, *Fate of the false Mott-Hubbard transition in two dimensions*, Phys. Rev. B **91** (2015) 125109.